Probing electroweak physics for all $B \to XM$ decays in the endpoint region

Junegone Chay,[1,*] Chul Kim,[2,†] Adam K. Leibovich,[2,‡] and Jure Zupan[3,4,§]

[1]*Department of Physics, Korea University, Seoul 136-701, Korea*
[2]*Department of Physics and Astronomy, University of Pittsburgh, Pennsylvania 15260, USA*
[3]*Department of Physics, University of Ljubljana, Jadranska 19, 1000 Ljubljana, Slovenia*
[4]*J. Stefan Institute, Jamova 39, P.O. Box 3000, 1001 Ljubljana, Slovenia*

Using soft-collinear effective theory we describe at leading order in $1/m_b$ all the semi-inclusive hadronic $B \to XM$ decays near the endpoint, where an energetic light meson M recoils against an inclusive jet X. Here we extend to the decays in which spectator quarks go into the jet X, and also include the decays involving η, η' mesons that receive additional contributions from gluonic operators. The predicted branching ratios and CP asymmetries depend on fewer hadronic parameters than the corresponding two-body B decays. This makes semi-inclusive hadronic $B \to XM$ decays a powerful probe of the potential nonperturbative nature of charming penguins as well as a useful probe of new physics effects in electroweak flavor changing transitions. A comparison with $B \to KX$ data from *BABAR* points to an enhanced charming penguin, albeit with large experimental errors.

I. INTRODUCTION

Recently *BABAR* made the first measurement of semi-inclusive $B \to KX$ branching ratios using fully reconstructed B decays [1]

$$\text{Br}(B^-/\bar{B}^0 \to K^- X) = (196^{+37+31}_{-34-30}) \times 10^{-6},$$
$$\text{Br}(B^-/\bar{B}^0 \to \bar{K}^0 X) = (154^{+55+55}_{-48-41}) \times 10^{-6}, \quad (1)$$

where a lower cut on the kaon momentum $p^*(K) > 2.34$ GeV in the B rest frame was imposed. This opens up the road for experimental explorations in hadronic semi-inclusive B decays, where for almost a decade the only observable probe has been $\text{Br}(B \to \eta' X)$, first determined by CLEO [2]. Averaging over the most recent measurements from *BABAR* [3] and CLEO [4] gives this branching ratio

$$\text{Br}(B \to \eta' X_s) = (420 \pm 94) \times 10^{-6} \quad (2)$$

for a lower cut on η' energy of $E_{\eta'} > 2.218$ GeV.

From the theoretical side semi-inclusive hadronic decays are very interesting since they are simpler, yet can still probe many of the questions that have been raised in the context of two-body B decays such as the perturbative and nonperturbative nature of charming penguins [5] and the search for new physics signals [6]. Theoretical simplification occurs in the endpoint region, where the energy of the light meson M is relatively close to the maximal energy, so that the isolated energetic meson M and the inclusive collinear hadronic jet X go in opposite directions. Incidentally, this is also the part of phase space that is most readily probed experimentally.

First predictions for the semi-inclusive hadronic decays $B \to XM$ in the endpoint region were given in Refs. [5,6] using the soft-collinear effective theory (SCET) [7–10] (for earlier works on semi-inclusive decays using different theoretical approaches see [11–18]). In the present work we go beyond Ref. [5] in several ways. First, because of the new experimental data on $B \to KX$ branching ratios in Eq. (1), we are able to discuss the size of charming penguins and include it in perturbative predictions. Second, contrary to Ref. [5] in which only decays where the spectator quark is part of the inclusive jet were considered, we extend the discussion to all semi-inclusive decays, including decays to η, η'. This is simplified by the fact that contributions where the spectator quark becomes part of the exclusive final state meson M are $1/m_b^2$ suppressed and can be neglected in our leading-order calculations. These contributions are schematically shown in Fig. 1(b) to be compared with the leading-order contributions in Fig. 1(a) (additional gluonic contributions are present for decays into η, η').

This means that the nonperturbative parameters ζ^{BM}, ζ_J^{BM}, connected to the $B \to M$ form factors, do not enter in the leading-order $B \to XM$ predictions, making them simpler than the predictions for the corresponding hadronic two-body B decays [19–25]. The presence of an inclusive collinear jet in the final state is described by a convolution of a nonperturbative shape function with a jet function. The latter arises in the matching of the full theory onto SCET$_I$ at the scale $p_X^2 \sim m_b \Lambda_{\text{QCD}}$. At leading order this convolution is the same as in $B \to X_s \gamma$ decays, so that many hadronic uncertainties cancel by taking ratios.

*chay@korea.ac.kr
†chk30@pitt.edu
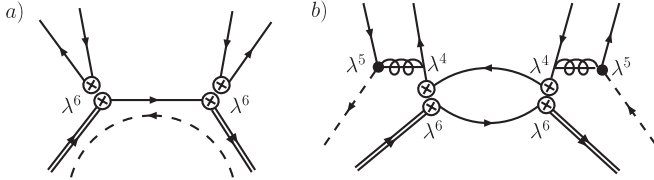‡akl2@pitt.edu
§jure.zupan@ijs.si

FIG. 1. Time-ordered products of the effective weak operators for the decay widths: (a) the leading-order contributions, (b) a subset of subleading spectator interactions discussed in Sec. II. The heavy quark fields are denoted by double lines, collinear quarks (gluons) by solid lines (overlaid with wiggly line), and soft quarks by dashed lines. The n hard-collinear quarks connecting the weak vertices and the $\bar{n}$ hard-collinear gluons [boosting the spectator in (b)] carry $p^2 \sim \Lambda m_b$ and are integrated out. The scaling of vertices is in $\lambda = \sqrt{\Lambda/m_b}$, cf. Sec. II.

The paper is organized as follows. In Sec. II we show the SCET power counting for the different possible decay contributions. This will allow us to include decays where the spectator could end up in the meson. We also discuss in this section the extra gluonic operators which contribute when the outgoing meson is an isosinglet meson. In Sec. III we briefly review the results of [5] and present the hard kernels for all semi-inclusive hadronic decays. In Sec. IV we discuss the production of η and η' mesons, where new gluonic operators are present at leading order in the power counting. In Sec. V we compare the predictions with data and then conclude in Sec. VI.

II. POWER COUNTING

We work at leading order in $1/m_b$ as in Ref. [5]. At this order it is fairly easy to modify the results of Ref. [5] to include the semi-inclusive decays in which the spectator can go to either the jet or the light meson. In particular contributions where the spectator quark is boosted to become part of the exclusive final state meson M are $1/m_b^2$ suppressed and can be neglected.

To show this we first explicitly power count different leading and subleading graphs in SCET$_\mathrm{I}$, where the expansion parameter is $\lambda = \sqrt{\Lambda/m_b}$. Order of the graph, λ^δ, is given simply by power counting the different vertices appearing in the graph [26]

$$\delta = 4 + \sum_k (k - 4)V_k, \qquad (3)$$

where V_k is the number of vertices that scale as λ^k (the above equation already assumes that there are no purely ultrasoft diagrams). Now consider the contribution where the spectator ends up in the jet as shown in Fig. 1(a). For this graph $V_6 = 2$ which gives a scaling

$$\delta_\mathrm{jet} = 4 + (6 - 4) \times 2 = 8. \qquad (4)$$

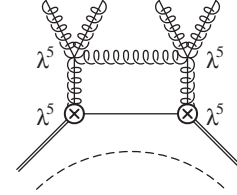After SCET$_\mathrm{I} \to$ SCET$_\mathrm{II}$ matching there is an additional

FIG. 2. Diagram that contributes to isosinglet meson production, which is of the same order as the leading diagram.

suppression of λ for each external collinear line, which results in a final power counting of $\lambda^{12} = (\Lambda_\mathrm{QCD}/m_b)^6$. This is the leading-order term for semi-inclusive hadronic B decays.

Next consider the contribution where the spectator ends up in the meson. A typical diagram is shown in Fig. 1(b) with $V_4 = 2$, $V_5 = 2$, and $V_6 = 2$, leading to

$$\delta_\mathrm{spect} = 4 + (4 - 4) \times 2 + (5 - 4) \times 2 + (6 - 4) \times 2$$
$$= 10. \qquad (5)$$

In addition to the usual λ suppression for each external collinear line in the matching SCET$_\mathrm{I} \to$ SCET$_\mathrm{II}$, however, this diagram is further suppressed due to the $p_\perp$ occurring in each of the λ^4 collinear vertices. Lowering $p_\perp$ to the SCET$_\mathrm{II}$ scaling gives an extra power of λ for both vertices. This is exactly the same suppression that makes the soft-overlap and the hard-scattering contributions in heavy-to-light decays of the same order as discussed in Ref. [27]. The diagram in Fig. 1(b) therefore scales as $\lambda^{16} = (\Lambda_\mathrm{QCD}/m_b)^8$ and thus is $1/m_b^2$ suppressed compared to the leading contribution and can be neglected in the leading-order analysis. Other possible diagrams in which the spectator ends up in the final meson give the same suppression and can also be neglected. Note that this does not mean that all spectator interactions are $1/m_b^2$ suppressed. In particular, annihilation contributions where the spectator quark annihilates with a collinear quark in the jet arise already at $1/m_b$ order as in $B \to X\gamma$ [28].

The decays into isosinglet mesons η, η' have additional contributions from gluonic operators such as the one shown in Fig. 2, for which $V_5 = 4$ and therefore

$$\delta_\mathrm{iso} = 4 + (5 - 4) \times 4 = 8, \qquad (6)$$

which is the same power suppression as the diagram in Fig. 1(a). After matching onto SCET$_\mathrm{II}$ this diagram then contributes at leading power, $(\Lambda_\mathrm{QCD}/m_b)^6$. Thus, to analyze isosinglet meson production, we must include new contributions, complicating the analysis. Isosinglet meson production will be discussed in Sec. IV.

III. THE FORMALISM

In this section we briefly review the results obtained in [5] while extending them to the full set of semi-inclusive
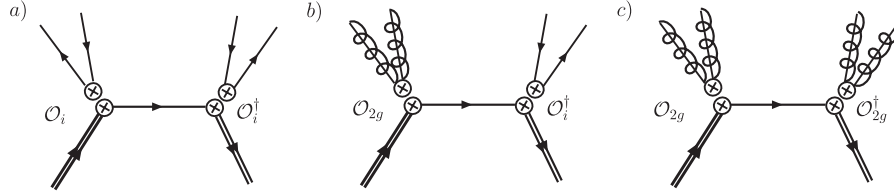
FIG. 3. Time-ordered products of $\mathcal{O}_i$ effective weak operators giving the decay widths through use of the optical theorem. The n collinear quarks connecting the weak vertices carry $p^2 \sim \Lambda m_b$ and are integrated out. The gluonic contributions (b) (with an additional mirror image not shown) and (c) contribute only to $B \to \eta^{(\prime)} X$ decays.

decays. Additional contributions that arise for decays with η or η' in the final state will be included in the next section. Barring those contributions, the decay rates of semi-inclusive B decays are obtained from the forward scattering amplitude of the time-ordered product of the heavy-to-light currents, as shown in Fig. 3. Because of disparate scales in the problem, a series of matchings on appropriate effective theories is performed. First, at the scale $\mu \sim m_b$ the standard effective weak Hamiltonian in full QCD for hadronic B decays [29] is matched onto the effective Hamiltonian in SCET$_{\rm I}$ by integrating out degrees of freedom of order m_b [19–21]. In the next step SCET$_{\rm I}$ is matched onto SCET$_{\rm II}$ by integrating out the degrees of freedom with $p^2 \sim m_b \Lambda$ [5]. As a result, the jet function is obtained, the discontinuity of which contributes to the semi-inclusive hadronic B decay rates. This jet function is the same as in $B \to X_s \gamma$ and will cancel once the ratio of decay rates is taken. The predictions for $B \to XM$ branching ratios normalized to Br$(B \to X_s \gamma)$ and for direct CP asymmetries in $B \to XM$ will thus depend only on perturbatively calculable hard kernels obtained from matching on SCET$_{\rm I}$ at $\mu \sim m_b$, and on the remaining nonperturbative parameters—light cone distribution amplitudes (LCDA) and the parameters describing nonperturbative charming penguins.

The hard kernels will depend on the Wilson coefficients $\mathcal{C}_i^p$ of the SCET$_{\rm I}$ weak Hamiltonian that is at leading order (LO) in $1/m_b$ given by [19–21]

$$H_I = \frac{2G_F}{\sqrt{2}} \sum_{p=u,c} \lambda_p^{(q)} \sum_{i=1}^{6,g} \mathcal{C}_i^p \otimes \mathcal{O}_i, \qquad (7)$$

where $\otimes$ denotes the convolution over collinear momenta fractions, while $\lambda_p^{(q)} = V_{pb} V_{pq}^*$ is the Cabibbo-Kobayashi-Maskawa (CKM) factor with $q = s$, d for $\Delta S = 1$, 0 transitions. The Wilson coefficients $\mathcal{C}_i^p$ are shown at leading order in Appendix A, and were calculated at next-to-leading order (NLO) in $\alpha_s(m_b)$ first in Refs. [23], and then in Ref. [19]. In our notation, the NLO Wilson coefficients can be found in Appendix A of Ref. [5]. The sum is over four-quark operators

$$\mathcal{O}_1 = [\bar{u}_n \slashed{n} P_L Y_n^\dagger b_v][\bar{q}_{\bar{n}} \slashed{n} P_L u_{\bar{n}}]_u,$$
$$\mathcal{O}_{2,3} = [\bar{q}_n \slashed{n} P_L Y_n^\dagger b_v][\bar{u}_{\bar{n}} \slashed{n} P_{L,R} u_{\bar{n}}]_u,$$
$$\mathcal{O}_4 = \sum_{q'} [\bar{q}'_n \slashed{n} P_L Y_n^\dagger b_v][\bar{q}_{\bar{n}} \slashed{n} P_L q'_{\bar{n}}]_u, \qquad (8)$$
$$\mathcal{O}_{5,6} = \sum_{q'} [\bar{q}_n \slashed{n} P_L Y_n^\dagger b_v][\bar{q}'_{\bar{n}} \slashed{n} P_{L,R} q'_{\bar{n}}]_u,$$

and the gluonic operators are (the trace is over color indices)

$$\mathcal{O}_{1g} = -\frac{m_b}{4\pi^2}[\bar{q}_n Y_{\bar{n}}^\dagger Y_{\bar{n}} \slashed{n} n \cdot P i g \mathcal{B}_{\bar{n}}^\perp P_R Y_n^\dagger b_v],$$
$$\mathcal{O}_{2g} = \frac{g^2 m_b}{4\pi^2}[\bar{q}_n \slashed{n} P_L Y_n^\dagger b_v] \text{Tr}[\mathcal{B}_{\bar{n}}^{\perp\mu} \mathcal{B}_{\bar{n}}^{\perp\nu}]_u i\epsilon_{\perp\mu\nu}, \qquad (9)$$

where the purely gluonic field $\mathcal{B}_{\bar{n}}^{\perp\mu}$ is related to the $(\bar{n}, \perp)$ component of the gluon field strength using the usual bracket prescription [20]

$$ig\mathcal{B}_{\bar{n}}^{\perp\mu} = \frac{1}{n \cdot P}[W_{\bar{n}}^\dagger [in \cdot D_{\bar{n}}, iD_{\bar{n}\perp}^\mu] W_{\bar{n}}]. \qquad (10)$$

The operators $\mathcal{O}_{1g,2g}$ contribute only to the decays with η, η' in the final state. We list the operator $\mathcal{O}_{2g}$ for completeness, in order to have expressions valid to LO in $1/m_b$ but to all order in $\alpha_s(m_b)$. When we discuss the phenomenology in Sec. V, we work at $O(\alpha_s(m_b))$. At this order $\mathcal{O}_{2g}$ has a vanishing matching coefficient [21] and thus does not contribute to the order that we are working.

The summation over q' in Eq. (8) includes u, d, and s quarks and $P_{L,R} = (1 \mp \gamma_5)/2$. The notation is the same as the one used in [5]. Thus $[\bar{q}_{\bar{n}} \slashed{n} P_L q_{\bar{n}}]_u = [\bar{q}_{\bar{n}} \delta(u - \frac{n \cdot \mathcal{P}^\dagger}{2E_M})\slashed{n} P_L q_{\bar{n}}]$, while gauge-invariant n and $\bar{n}$ collinear quark fields $q_n = W_n^\dagger \xi_n^{(q)}$ and $q_{\bar{n}} = W_{\bar{n}}^\dagger \xi_{\bar{n}}^{(q)}$ already contain the collinear Wilson lines. The ultrasoft (usoft) Wilson line in the n direction, Y_n, arises after the redefinition of the collinear fields to decouple collinear and usoft degrees of freedom [10].

This decoupling implies that the operators in Eqs. (8) and (9) factorize into currents $J_C = (\bar{q}_{\bar{n}} \slashed{n} \Gamma q'_{\bar{n}})$ and $J_H = (\bar{q}_n \slashed{n} P_L Y_n^\dagger b_v)$ which do not exchange soft gluons. The

matrix elements of $\bar{n}$ currents $\langle M|J_C|0\rangle$ are expressed in terms of LCDA, while the time-ordered product of heavy-to-light currents,

$$T(E_M) = \frac{i}{m_B}\int d^4z e^{-ip_M\cdot z}\langle B|TJ_H^\dagger(z)J_H(0)|B\rangle, \quad (11)$$

leads to a convolution of shape, $f(l_+)$, and jet functions, J_P, [5]

$$\frac{1}{\pi}\,\text{Im}\,T(E_M) = 2\int_{-m_b+2E_M}^{\bar{\Lambda}} dl_+ f(l_+)$$
$$\times\left[-\frac{1}{\pi}\text{Im}\,J_P(m_b - 2E_M + l_+ + i\epsilon)\right]$$
$$\equiv \frac{2}{m_b}\mathcal{S}(E_M,\mu_0), \quad (12)$$

where $l_+ = n\cdot l$ is the soft momentum conjugate to the $\bar{n}\cdot z = z_-$ spatial component. Using the optical theorem this is then related to the $B\to XM$ decay rate giving

$$\frac{d\Gamma}{dE_M}(B\to XM) = \frac{G_F^2}{8\pi}m_b^2 x_M^3\mathcal{S}(x_M,\mu_0)|h_M^{(q)}|^2 + \cdots, \quad (13)$$

where $x_M = 2E_M/m_b \simeq 1$. The ellipses represent nonperturbative charming penguin contributions given explicitly below, while $h_M^{(q)}$ is the convolution of the hard kernel and the LCDA

$$h_M^{(q)} = f_M\int_0^1 du\phi_M(u)[\lambda_u^{(q)}T_{M,u}^{(q)}(u) + \lambda_c^{(q)}T_{M,c}^{(q)}(u)]. \quad (14)$$

Here $\phi_M(u)$ is the light meson LCDA, f_M the decay constant, $\lambda_p^{(q)} = V_{pb}V_{pq}^*$ the CKM elements, while the perturbatively calculable hard kernels $T_{M,p}^{(q)}$ are given in Tables I and II for $\Delta S = 1, 0$ ($q = s, d$), respectively.

The nonperturbative function $\mathcal{S}$ denoting the convolution of shape and jet functions is exactly the same as the one appearing in the prediction for the $B\to X_s\gamma$ rate in the endpoint region at LO in $1/m_b$. In the ratio with $\Gamma(B\to X_s\gamma)$ it thus cancels out, giving

$$\frac{d\Gamma(\bar{B}\to MX)/dE_M}{d\Gamma(\bar{B}\to X_s\gamma)/dE_\gamma} = \frac{2\pi^3}{\alpha m_b^2}\frac{(|h_M^{(q)}|^2 + 2\text{Re}[\lambda_c^{(q)}c_{cc}P_{cc}^M(h_M^{(q)})^*] + |\lambda_c^{(q)}c_{cc}|^2\mathcal{P}_{cc}^M)}{|\lambda_t^{(s)}C_\gamma(c_9^{\text{eff}} + 1/2c_{12}^{\text{eff}})|^2}, \quad (15)$$

TABLE I. Hard kernels $\mathcal{T}_{M,p}'^{(s)}$ with $p = u, c$ for $\Delta S = 1$ semi-inclusive $B^-/\bar{B}^0/\bar{B}_s^0 \to XM$ decays. The NLO Wilson coefficients $\mathcal{C}_i^p$ are given in Appendix A of [5]. For the additional gluonic contributions to decays with $\eta_{q,s}$ see Sec. IV.

$B^- \to MX$	$\bar{B}^0 \to MX$	$\bar{B}_s^0 \to MX$	$T_{M,p}^{(s)}$
$K^{(*)-}X_{u\bar{u}}^0$	$K^{(*)-}X_{u\bar{d}}^+$	$K^{(*)-}X_{u\bar{s}}^+$	$\mathcal{C}_1^p + \mathcal{C}_4^p$
$\bar{K}^{(*)0}X_{d\bar{u}}^-$	$\bar{K}^{(*)0}X_{d\bar{d}}^0$	$\bar{K}^{(*)0}X_{d\bar{s}}^0$	$\mathcal{C}_4^p$
$\phi X_{s\bar{u}}^-$	$\phi X_{s\bar{d}}^0$	$\phi X_{s\bar{s}}^0$	$\mathcal{C}_4^p + \mathcal{C}_5 + \mathcal{C}_6$
$\eta_s X_{s\bar{u}}^-$	$\eta_s X_{s\bar{d}}^0$	$\eta_s X_{s\bar{s}}^0$	$\mathcal{C}_4^p + \mathcal{C}_5 - \mathcal{C}_6$
$\omega X_{s\bar{u}}^-$	$\omega X_{s\bar{d}}^0$	$\omega X_{s\bar{s}}^0$	$(\mathcal{C}_2^p + \mathcal{C}_3 + 2\mathcal{C}_5 + 2\mathcal{C}_6)/\sqrt{2}$
$\eta_q X_{s\bar{u}}^-$	$\eta_q X_{s\bar{d}}^0$	$\eta_q X_{s\bar{s}}^0$	$(\mathcal{C}_2^p - \mathcal{C}_3 + 2\mathcal{C}_5 - 2\mathcal{C}_6)/\sqrt{2}$
$\pi^0 X_{s\bar{u}}^-, \rho^0 X_{s\bar{u}}^-$	$\pi^0 X_{s\bar{d}}^0, \rho^0 X_{s\bar{d}}^0$	$\pi^0 X_{s\bar{s}}^0, \rho^0 X_{s\bar{s}}^0$	$(\mathcal{C}_2^p \mp \mathcal{C}_3)/\sqrt{2}$

TABLE II. Hard kernels $\mathcal{T}_{M,p}^{(d)}$ with $p = u, c$ for $\Delta S = 0$ semi-inclusive $B^-/\bar{B}^0/\bar{B}_s^0 \to XM$ decays. The summation over $p = u, c$ is implied. The NLO Wilson coefficients $\mathcal{C}_i^p$ are given in Appendix A of [5]. For the additional gluonic contributions to decays with $\eta_{q,s}$ see Sec. IV.

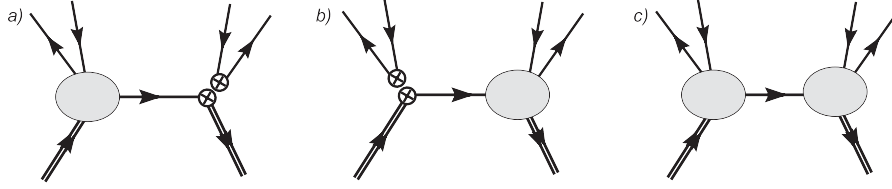| $B^- \to MX$	$\bar{B}^0 \to MX$	$\bar{B}_s^0 \to MX$	$T_{M,p}^{(d)}$
$\pi^- X_{u\bar{u}}^0, \rho^- X_{u\bar{u}}^0$	$\pi^- X_{u\bar{d}}^+, \rho^- X_{u\bar{d}}^+$	$\pi^- X_{u\bar{s}}^+, \rho^- X_{u\bar{s}}^+$	$\mathcal{C}_1^p + \mathcal{C}_4^p$
$\pi^0 X_{d\bar{u}}^-, \rho^0 X_{d\bar{u}}^-$	$\pi^0 X_{d\bar{d}}^0, \rho^0 X_{d\bar{d}}^0$	$\pi^0 X_{d\bar{s}}^0, \rho^0 X_{d\bar{s}}^0$	$(\mathcal{C}_2^p - \mathcal{C}_4^p \mp \mathcal{C}_3)/\sqrt{2}$
$K^{(*)0}X_{s\bar{u}}^-$	$K^{(*)0}X_{s\bar{d}}^0$	$K^{(*)0}X_{s\bar{s}}^0$	$\mathcal{C}_4^p$
$\omega X_{d\bar{u}}^-$	$\omega X_{d\bar{d}}^0$	$\omega X_{d\bar{s}}^0$	$(\mathcal{C}_2^p + \mathcal{C}_4^p + \mathcal{C}_3 + 2\mathcal{C}_5 + 2\mathcal{C}_6)/\sqrt{2}$
$\eta_q X_{d\bar{u}}^-$	$\eta_q X_{d\bar{d}}^0$	$\eta_q X_{d\bar{s}}^0$	$(\mathcal{C}_2^p + \mathcal{C}_4^p - \mathcal{C}_3 + 2\mathcal{C}_5 - 2\mathcal{C}_6)/\sqrt{2}$
$\phi X_{d\bar{u}}^-$	$\phi X_{d\bar{d}}^0$	$\phi X_{d\bar{s}}^0$	$\mathcal{C}_5 + \mathcal{C}_6$
$\eta_s X_{d\bar{u}}^-$	$\eta_s X_{d\bar{d}}^0$	$\eta_s X_{d\bar{s}}^0$	$\mathcal{C}_5 - \mathcal{C}_6$

FIG. 4.   Charming penguin contributions: the contributions from (a) and (b) are proportional to p_{cc}^M and p_{cc}^{M*}, respectively, while the contribution from (c) gives $\mathcal{P}_{cc}^M$. The blobs represent nonperturbative charming penguins.

where one sets $E_\gamma = E_M$. The SCET Wilson coefficients are $c_9^{\text{eff}} = 1$, $c_{12}^{\text{eff}} = 0$ at LO with the NLO calculated in [8], while C_γ is given e.g. in Eq. (13) of [28].

The coefficients p_{cc}^M and $\mathcal{P}_{cc}^M$ parametrize possible nonperturbative charming penguin contributions.[1] They depend on the valence quark structure of both M and the jet X, but we suppress this dependence in the notation. They are zero if the charming penguin contributions are purely perturbative. However, the uncalculated higher-order perturbative pieces can mimic their effect, making them differ slightly from zero. The complex parameter p_{cc}^M describes the interference of the nonperturbative charming penguin with the perturbative hard kernels, shown in Fig. 4(a). The positive real parameter $\mathcal{P}_{cc}^M$ in Eq. (15) on the other hand describes the square of the nonperturbative charming penguin contributions shown in Fig. 4(c). If hard kernels dominate the amplitudes, the term with p_{cc}^M in Eq. (15) is subleading, while the $\mathcal{P}_{cc}^M$ term is even more suppressed and can be neglected as was done in [5]. It should be kept, however, if nonperturbative charming penguins are sizable. Since the present data are inconclusive we keep both terms in Eq. (15). When estimating the size of the nonperturbative contributions, as a rule of thumb we will take $(p_{cc}^M)^2 \sim \mathcal{P}_{cc}^M$. Further information on the structure of p_{cc}^M, $\mathcal{P}_{cc}^M$ can be obtained in the $m_c \to \infty$ limit [5]. Finally, the coefficient c_{cc} multiplying the nonperturbative charming penguin parameters in Eq. (15) is equal to the coefficient of $\mathcal{C}_4^c$ in Tables I and II (i.e., it is $c_{cc} = 1$ for $B^- \to \pi^- X_{u\bar{u}}^0$ and $c_{cc} = -1/\sqrt{2}$ for $B^- \to \pi^0 X_{d\bar{u}}^-$ so that p_{cc}^M in both cases equals p_{cc}^π).

In the phenomenological analysis of our results in Sec. V we give numerical estimates for direct CP asymmetries

$$
\begin{aligned}
&A_{CP}(\bar{B} \to XM) \\
&\quad = \frac{d\Gamma(\bar{B} \to XM)/dE_M - d\Gamma(B \to XM)/dE_M}{d\Gamma(\bar{B} \to XM)/dE_M + d\Gamma(B \to XM)/dE_M},
\end{aligned}
\tag{16}
$$

and CP averaged branching ratios. In terms of hard kernels and nonperturbative charming penguin parameters the direct CP asymmetry is

---

$$
A_{CP}(\bar{B} \to XM) = \frac{-2\operatorname{Im}(\lambda_u^{(q)} \lambda_c^{(q)*})}{|A(\bar{B} \to XM)|^2} \operatorname{Im}[T(P + c_{cc} p_{cc}^M)^*],
\tag{17}
$$

and the CP averaged decay width normalized to $B \to X_s \gamma$ is

$$
\frac{d\Gamma_{CP}(\bar{B} \to MX)/dE_M}{d\Gamma(\bar{B} \to X_s\gamma)/dE_\gamma} = \frac{2\pi^3}{\alpha m_b^2} \frac{|A(\bar{B} \to XM)|^2}{|\lambda_t^{(s)} C_\gamma (c_9^{\text{eff}} + 1/2 c_{12}^{\text{eff}})|^2},
\tag{18}
$$

where

$$
\begin{aligned}
|A(\bar{B} \to XM)|^2 = {} & |\lambda_u^{(q)}|^2 |T|^2 + 2\operatorname{Re}(\lambda_u^{(q)} \lambda_c^{(q)*}) \\
& \times \operatorname{Re}[T(P + c_{cc} p_{cc}^M)^*] \\
& + |\lambda_c^{(q)}|^2 [|P|^2 + 2\operatorname{Re}(c_{cc} p_{cc}^M P^*) \\
& + c_{cc}^2 \mathcal{P}_{cc}^M].
\end{aligned}
\tag{19}
$$

Above a shorthand notation for the perturbative "tree" and "penguin" contributions

$$
\begin{aligned}
T &= \int_0^1 du\, f_M \phi_M(u) T_{M,u}^{(q)}(u), \\
P &= \int_0^1 du\, f_M \phi_M(u) T_{M,c}^{(q)}(u),
\end{aligned}
\tag{20}
$$

has been used, dropping in the notation the dependence on $\bar{B} \to XM$.

IV. THE DECAYS INVOLVING η, η'

In order to describe $B \to \eta^{(')} X$ decays several modifications of the results in the previous section are needed: (i) $\eta - \eta'$ mixing needs to be taken into account and (ii) there are additional contributions from gluonic operators $\mathcal{O}_{1g,2g}$ as shown in Figs. 3 and 5 [operators $\mathcal{O}_{1g,2g}$ are defined in Eq. (9)]. To describe matrix elements involving gluonic operators we introduce the gluonic LCDA [30,31]

$$
i\epsilon_{\perp\mu\nu}\langle P(p)|\operatorname{Tr}[\mathcal{B}_{\bar{n}}^{\perp\mu} \mathcal{B}_{\bar{n}}^{\perp\nu}]_u|0\rangle = \frac{i}{4}\sqrt{C_F} f_P^1 \bar{\Phi}_P^g(u),
\tag{21}
$$

where the isosinglet decay constant is the same one that appears in the matrix elements of quark bilinears

$$
\langle P(p)|[\bar{q}_{\bar{n}} \slashed{n} \gamma_5 T_{1,8} q_{\bar{n}}]_u|0\rangle = -2iEf_P^{1,8} \phi_P^{1,8}(u),
\tag{22}
$$

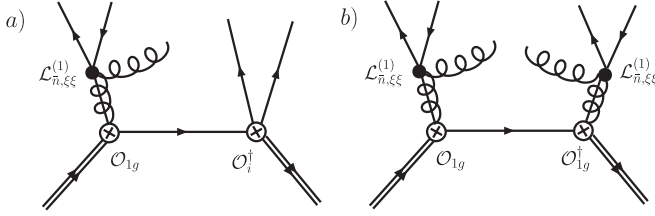with $T_8 = \lambda_8/\sqrt{2}$, $T_1 = 1/\sqrt{3}$ diagonal 3×3 matrices in

FIG. 5. The contributions of $\mathcal{O}_{1g}$ operator to $B \to MX_q$ decays. The mirror image of diagram (a) is not shown as well as not the diagrams with $\mathcal{L}^{(1)}_{\bar{n},\xi\xi}$ replaced by $\mathcal{L}^{(1)}_{\bar{n},cg}$, cf. Fig. 6.

u, d, s flavor space. The flavor singlet LCDA $\phi_P^1(u)$ mixes with the gluonic LCDA $\bar{\Phi}_P^g(u)$ under RG running [32], while $\phi_P^8(u)$ does not. For future reference we also quote explicitly $f_{\eta_q}^1 = \sqrt{2/3} f_{\eta_q}$, $f_{\eta_s}^1 = f_{\eta_s}/\sqrt{3}$, while $f_P^1 = 0$ for other pseudoscalars that do not have flavor singlet component. Here f_{η_q} and f_{η_s} are the decay constants corresponding to $\bar{q}q = (\bar{u}u + \bar{d}d)/\sqrt{2}$ and $\bar{s}s$ axial currents, respectively (and are equal in the SU(3) limit, cf. also (25) below).

The parametrizations of matrix elements (21) and (22) do not involve any assumptions; however they are too general for the limited amount of data available at present. To reduce the number of unknowns we use the Feldmann-Kroll-Stech (FKS) mixing scheme [33] to describe $\eta - \eta'$ mixing in which the mass eigenstates η, η' are related to the flavor basis through

$$\eta = \eta_q \cos\varphi - \eta_s \sin\varphi, \qquad \eta' = \eta_q \sin\varphi + \eta_s \cos\varphi, \tag{23}$$

with $\varphi = (39.3 \pm 1.0)°$ and $\eta_q = (\eta_u + \eta_d)/\sqrt{2}$. The working assumptions of the FKS scheme are that LCDA do not depend on the meson so that

$$\phi_P^{1,8}(u) = \phi^{1,8}(u), \qquad \bar{\Phi}_P^g(u) = \bar{\Phi}^g(u), \tag{24}$$

and that Okubo-Zweig-Iizuka (OZI) suppression is effective. This last requirement is most transparent in the η_q, η_s, g basis instead of the 1, 8, g basis used above. In it we have

$$\langle \eta_q(p)| \frac{1}{\sqrt{2}} ([\bar{u}_{\bar{n}} \slashed{n} \gamma_5 u_{\bar{n}}]_u + [\bar{d}_{\bar{n}} \slashed{n} \gamma_5 d_{\bar{n}}]_u)|0\rangle = -2iEf_{\eta_q} \phi_{\eta_q}(u), \qquad \langle \eta_s(p)|[\bar{s}_{\bar{n}} \slashed{n} \gamma_5 s_{\bar{n}}]_u|0\rangle = -2iEf_{\eta_s} \phi_{\eta_s}(u), \tag{25}$$

with $\phi_{\eta_s}(u) = [2\phi^8(u) + \phi^1(u)]/3$ and $\phi_{\eta_q}(u) = [2\phi^1(u) + \phi^8(u)]/3$. The OZI suppressed matrix elements on the other hand are

$$\langle \eta_s(p)| \frac{1}{\sqrt{2}} ([\bar{u}_{\bar{n}} \slashed{n} \gamma_5 u_{\bar{n}}]_u + [\bar{d}_{\bar{n}} \slashed{n} \gamma_5 d_{\bar{n}}]_u)|0\rangle = -2iEf_{\eta_s} \phi_{\text{opp}}(u), \qquad \langle \eta_q(p)|[\bar{s}_{\bar{n}} \slashed{n} \gamma_5 s_{\bar{n}}]_u|0\rangle = -2iEf_{\eta_q} \phi_{\text{opp}}(u), \tag{26}$$

where $\phi_{\text{opp}}(u) = \sqrt{2}[\phi^1(u) - \phi^8(u)]/3$ and is negligible as long as $\phi^1(u) \simeq \phi^8(u)$. This relation is exact for asymptotic forms of LCDA, while it can only be approximate for physical values of μ since $\phi^1(u)$ and $\phi^8(u)$ have different RG runnings, spoiling the relation for smaller values of μ. Phenomenologically, however, for μ above 1 GeV the relation is well obeyed at a percent level [30].

We are now ready to write down the results for contributions to $B \to \eta(\eta')X$ decays corresponding to Figs. 3 and 4. These are described by Eq. (15) but with $h_M^{(q)}$ and charming penguin parameters as given below. Utilizing the FKS scheme with Eq. (25) and setting the OZI suppressed matrix elements Eq. (26) to zero, the $h_M^{(q)}$ functions in Eq. (15) are

$$h_\eta^{(q)} = \cos\varphi f_{\eta_q} \phi_{\eta_q} \otimes \lambda_p^{(q)} T_{\eta_q,p}^{(q)} - \sin\varphi f_{\eta_s} \phi_{\eta_s} \otimes \lambda_p^{(q)} T_{\eta_s,p}^{(q)} + h_\eta^g, \tag{27}$$

$$h_{\eta'}^{(q)} = \sin\varphi f_{\eta_q} \phi_{\eta_q} \otimes \lambda_p^{(q)} T_{\eta_q,p}^{(q)} + \cos\varphi f_{\eta_s} \phi_{\eta_s} \otimes \lambda_p^{(q)} T_{\eta_s,p}^{(q)} + h_{\eta'}^g, \tag{28}$$

where $\otimes$ denotes a convolution, while $T_{\eta_{q,s},p}^{(q)}$ are listed in Tables I and II and the sum over $p = u, c$ is understood.

The gluonic contributions h_M^g coming from the $\mathcal{O}_{2g}$ operator insertions as shown in Figs. 3(b) and 3(c), are zero to NLO in $\alpha_s(m_b)$, i.e. to the order we are working. Explicitly, they are

$$h_{\eta_{s,q}}^g = -\lambda_t^{(s)} \frac{\sqrt{C_F}}{2} f_{\eta_{s,q}}^1 \bar{\Phi}_{\eta_{s,q}}^g(u) \otimes \mathcal{C}_{2g}(u), \tag{29}$$

for $\Delta S = 1$ decays $B_{q'} \to \eta_{s,q} X_{s\bar{q}'}$, while for $\Delta S = 0$ decays $B_{q'} \to \eta_{s,q} X_{d\bar{q}'}$ we need to replace $\lambda_t^{(s)} \to \lambda_t^{(d)}$. The expressions for η, η' final states are easily obtained using (23). As already stated, $\mathcal{C}_{2g}(u) = 0$ at NLO in $\alpha_s(m_b)$.

For the charming penguin parameters in Eq. (15), we make the following replacements for $\Delta S = 1$ transitions

$$c_{cc} p_{cc}^\eta \to -\sin\varphi p_{cc}^{\eta_s}, \qquad c_{cc}^2 \mathcal{P}_{cc}^\eta \to \sin^2\varphi \mathcal{P}_{cc}^{\eta_s},$$
$$c_{cc} p_{cc}^{\eta'} \to \cos\varphi p_{cc}^{\eta_s}, \qquad c_{cc}^2 \mathcal{P}_{cc}^{\eta'} \to \cos^2\varphi \mathcal{P}_{cc}^{\eta_s}, \tag{30}$$

and for $\Delta S = 0$ transitions

$$c_{cc} p_{cc}^\eta \to \frac{\cos\varphi}{\sqrt{2}} p_{cc}^{\eta_q}, \qquad c_{cc}^2 \mathcal{P}_{cc}^\eta \to \frac{\cos^2\varphi}{2} \mathcal{P}_{cc}^{\eta_q},$$
$$c_{cc} p_{cc}^{\eta'} \to \frac{\sin\varphi}{\sqrt{2}} p_{cc}^{\eta_q}, \qquad c_{cc}^2 \mathcal{P}_{cc}^{\eta'} \to \frac{\sin^2\varphi}{2} \mathcal{P}_{cc}^{\eta_q}. \tag{31}$$
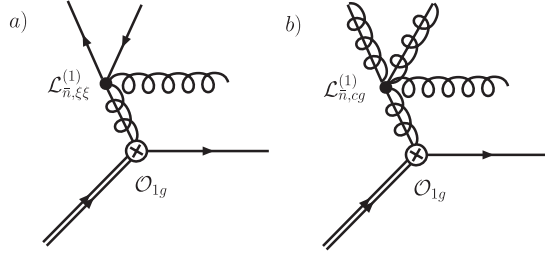
FIG. 6. Time-ordered products between $\mathcal{O}_{1g}$ and the subleading interaction terms in the SCET Lagrangian. The soft gluon (curly line) is absorbed in a definition of new B meson shape function f_g. The intermediate hard-collinear gluon has off-shellness $\sim m_b \Lambda$ and is integrated out. At LO in $\alpha_s(\sqrt{\Lambda m_b})$ diagram (b) does not contribute because of the antisymmetry of gluonic LCDA.

We next move to the contributions from the $\mathcal{O}_{1g}$ operator, shown in Fig. 5. These contributions lead to a modified factorization between n and $\bar{n}$ degrees of freedom because of the additional soft gluon that is emitted at a lightlike separation from the weak vertex in the $\bar{n}$ direction. Relegating the details to Appendix B, we quote here only the main results starting with the T products in Fig. 6

$$\mathcal{G}_{\xi\xi(cg)} = \langle MX | i \int d^4x T\{\mathcal{O}_{1g}(0), \mathcal{L}_{\xi\xi(cg)}^{(1)}(x)\} | B \rangle. \quad (32)$$

Then $\mathcal{G}_{\xi\xi} + \mathcal{G}_{cg}$ describes the contribution of the operator $\mathcal{O}_g$ to the decay into a color-singlet state.

In the $\text{SCET}_I \to \text{SCET}_{II}$ matching the intermediate hard-collinear gluon carrying $p^2 \sim \Lambda m_b$ is integrated out leading, respectively, to the jet functions $J_1(u, k_-)$ and $J_g(u, k_-)$ for the diagrams in Figs. 6(a) and 6(b). Following the usual redefinition of fields the $\bar{n}$ collinear quark (gluon) lines decouple from the soft fields [10] and lead to quark (gluon) LCDA after taking the matrix element. The soft Wilson lines $Y_{\bar{n}}$ arising from the field redefinition and the soft gluon field emitted at x are taken to be part of the heavy-to-light current

$$\tilde{J}_H(0, x_+) = \bar{q}_n Y_n^\dagger Y_{\bar{n}}(0) \slashed{n} g \mathcal{A}_{\text{us}}^\perp(x_+) P_R Y_{\bar{n}}^\dagger b_v(0), \quad (33)$$

where we define

$$g \mathcal{A}_{\text{us}}^{\perp\mu} = [Y_{\bar{n}}^\dagger i D_{\text{us}}^{\perp\mu} Y_{\bar{n}}]. \quad (34)$$

Note that the heavy-to-light current $\tilde{J}_H$ depends on x_+, since the soft gluon gets emitted away from the weak vertex. The $\mathcal{O}_{1g}$ contribution to the $B \to MX$ matrix element then takes a form of a convolution over both the soft momentum k_- (conjugate to the position x_+) and the hard momentum fraction $u p_M$,

$$\mathcal{G}_{\xi\xi} + \mathcal{G}_{cg} = -i \int du \int \frac{dk_- dx_+}{4\pi} e^{-ik_- x_+/2} F^M(k_-, u)$$
$$\times \langle X | \tilde{J}_H(0, x_+) | B \rangle. \quad (35)$$

The hard-collinear kernel multiplied by the LCDA is explicitly

$$F^M(k_-, u) = \frac{\alpha_s m_b}{4\pi} \left\{ f_M \phi_M(u) \left[\frac{J_1(u, k_-)}{u} - \frac{J_1(\bar{u}, -k_-)^*}{\bar{u}} \right] \right.$$
$$\left. + \sqrt{C_F} f_M^1 \bar{\Phi}_M^g(u) J_g(u, k_-) \right\}, \quad (36)$$

and is in general both a function of the $\bar{n}$ momentum fraction u and the soft momentum k_-. At tree level, however, it is a simple product of functions that depend only on u and only on k_-,

$$F^M(k_-, u)|_{\text{tree}} = \frac{\alpha_s m_b}{4\pi} f_M \phi_M(u) \left(\frac{1}{u} + \frac{1}{\bar{u}} \right) J_1(k_-) \bigg|_{\text{tree}}, \quad (37)$$

since $J_1(u, k_-)|_{\text{tree}} = J_1(k_-)|_{\text{tree}} = 1/(Nk_-)$ and $J_g(u, k_-)|_{\text{tree}} = 1/k_-$ are independent of u. Furthermore, since $\bar{\Phi}_P^g(u)$ is antisymmetric, $\bar{\Phi}_P^g(u) = -\bar{\Phi}_P^g(\bar{u})$, the contribution from $J_g(u, k_-)$ vanishes at this order.

Therefore at least at leading order in $\alpha_s(\sqrt{\Lambda m_b})$ the additional gluonic contributions can be cast in the same form as the expressions for the decay widths for nonisosinglet final states, Eq. (13), by moving the u-dependent part into the definition of hard kernels, while including the dependence on k_- in the definition of the modified heavy-to-light current

$$\tilde{\mathcal{J}}(0) = \int \frac{dk_- dx_+}{4\pi} e^{-ik_- x_+/2} \tilde{J}_H(0, x_+) J_1(k_-)|_{\text{tree}}. \quad (38)$$

Because of this simplification we will show in this section only the result for $B \to XM$ decay width at leading order in $\alpha_s(\sqrt{\Lambda m_b})$, while the result valid to all orders in $\alpha_s(\sqrt{\Lambda m_b})$ is given in Appendix B.

As in Sec. III we relate the $B \to XM$ decay width to the time-ordered product of heavy currents using the optical theorem. We denote the T-product coming from a single $\mathcal{O}_{1g}$ insertion, shown in Fig. 5(a), as

$$\tilde{T}_g(E_M) = \frac{i}{m_b} \int d^4z \langle B | T J_H^\dagger(z) \tilde{\mathcal{J}}(0) | B \rangle, \quad (39)$$

where $J_H(z) = e^{i(\tilde{p} - m_b v) \cdot z} (\bar{q}_n \slashed{n} P_L Y_n^\dagger b_v)(z)$. For the contribution coming from two insertions of $\mathcal{O}_{1g}$, shown in Fig. 5(b), we similarly define

$$\tilde{T}_{gg}(E_M) = \frac{i}{m_b} \int d^4z \langle B | T \tilde{\mathcal{J}}^\dagger(z) \tilde{\mathcal{J}}(0) | B \rangle. \quad (40)$$

In evaluating the time-ordered product $\tilde{T}_g(E_M)$ we use the fact that n collinear quark fields do not exchange any soft gluons at LO in $1/m_b$ with the other fields in the T-product. Using the standard definition of the n-collinear jet function,

$$\langle 0|Tq_n(z)\bar{q}_n(0)|0\rangle = i\frac{\rlap{/}{n}}{2}\delta(z_+)\delta^2(z_\perp)$$
$$\times \int \frac{d\kappa_+}{2\pi} e^{-i\kappa_+ z_-/2} J_P(\kappa_+ + i\epsilon), \tag{41}$$

and a shape function that, unlike $f(l_+)$ in Eq. (12), depends on two soft momenta because of the additional nonlocal structure present in $\tilde{\mathcal{J}}$ due to $\mathcal{A}_{\mathrm{us}}$,

$$\int dl_+ e^{il_+ z/2} \int dr_- e^{ir_- x_+/2} f_g(l_+, r_-)$$
$$= \langle B_v|\bar{b}_v Y_n(z_-) Y_{\bar{n}}^\dagger(0)\rlap{/}{n}g\mathcal{A}_{\mathrm{us}}^\perp(x_+) P_R Y_{\bar{n}}^\dagger b_v(0)|B_v\rangle, \tag{42}$$

the discontinuity of $\tilde{T}_g(E_M)$ with respect to the intermediate states is given by

$$\mathrm{Disc}.\tilde{T}_g(E_M) = 2\int dl_+ dr_-$$
$$\times \mathrm{Im}\left[-\frac{1}{\pi} J_P(l_+ + m_b - 2E_M + i\epsilon)\right]$$
$$\times f_g(l_+, r_-)J_1(r_-)|_{\mathrm{tree}}$$
$$\equiv \frac{2}{m_b}\mathcal{S}_g(E_M, \mu_0). \tag{43}$$

Note that the new shape function $f_g(l_+, r_-)$ can be in general complex, hence $\mathcal{S}_g$ can also be complex. However for decay rates, the complex conjugate should be added and the decay rates become real.

Using the optical theorem the contribution to the decay width from one insertion of $\mathcal{O}_{1g}$ at LO in $\alpha_s(\sqrt{\Lambda m_b})$, with the contribution of the mirror image of Fig. 5(a), is therefore

$$\left(\frac{d\Gamma}{dE_M}\right)_g\bigg|_{\mathrm{tree}} = \frac{G_F^2}{4\pi} m_b^2 x_M^2 f_M^2 2\mathrm{Re}\bigg\{ (\phi_M \otimes \lambda_p^{(q)} T_{M,p}^{(q)})^*$$
$$\times \left[\phi_M \otimes \lambda_t^{(q)} \mathcal{C}_{1g} \frac{\alpha_s}{4\pi}\left(\frac{1}{u} + \frac{1}{\bar{u}}\right)\right]$$
$$\times \mathcal{S}_g(E_M, \mu_0)\bigg\}, \tag{44}$$

where $\mathcal{C}_{1g}$ is the Wilson coefficient of $\mathcal{O}_{1g}$, which is 1 at leading order. This expression is similar to Eq. (13). The hard kernels (convoluted with LCDA) in the curly brackets do not depend on soft momenta k_- and similarly the nonperturbative "shape" function $\mathcal{S}_g$ does not depend on the large momenta fractions u. This factorization of the u and k_- dependence is a consequence of a special form of F^M at leading order in $\alpha_s(\sqrt{\Lambda m_b})$, Eq. (37), and may not be present at higher orders, cf. Eq. (36).

The contribution $\tilde{T}_{gg}$, Eq. (40), coming from two insertions of $\mathcal{O}_{1g}$ leads to a shape function that depends on three soft momenta because of two soft gluon insertions

$$\int dl_+ e^{il_+ z_-/2} \int dr_- e^{ir_- x_+/2} \int ds_- e^{is_- y_+/2} f_{gg}(l_+, r_-, s_-)$$
$$= \langle B_v|\bar{b}_v Y_{\bar{n}}(z_-)g\mathcal{A}_{\mathrm{us}}^\perp(y_+) Y_{\bar{n}}^\dagger Y_n(z_-) Y_n^\dagger Y_{\bar{n}}(0)\rlap{/}{n}g\mathcal{A}_{\mathrm{us}}^\perp(x_+)$$
$$\times P_R Y_{\bar{n}}^\dagger b_v(0)|B_v\rangle. \tag{45}$$

This gives a new nonperturbative shape function by taking the discontinuity

$$\mathrm{Disc}.\tilde{T}_{gg}(E_M) = 2\int dl_+ dr_- ds_-$$
$$\times \mathrm{Im}\left[-\frac{1}{\pi} J_P(l_+ + m_b - 2E_M + i\epsilon)\right]$$
$$\times J_1(r_-)J_1(s_-)^* f_{gg}(l_+, r_-, s_-)$$
$$\equiv \frac{2}{m_b}\mathcal{S}_{gg}(E_M, \mu_0), \tag{46}$$

which then enters the prediction for the contribution of double $\mathcal{O}_{1g}$ insertion to the decay width

$$\left(\frac{d\Gamma}{dE_M}\right)_{gg}\bigg|_{\mathrm{tree}} = \frac{G_F^2}{2\pi} m_b^2 x_M f_M^2 \mathcal{S}_{gg}(E_M, \mu_0)$$
$$\times \left| \lambda_t^{(q)} \mathcal{C}_{1g} \int du\phi_M(u)\frac{\alpha_s}{4\pi}\left(\frac{1}{u} + \frac{1}{\bar{u}}\right)\right|^2. \tag{47}$$

Note that f_{gg} and $\mathcal{S}_{gg}$ are real in contrast to f_g and $\mathcal{S}_g$.

To recapitulate, the prediction for the $B \to \eta(\eta')X$ decay widths at LO in $1/m_b$ is given by

$$\frac{d\Gamma}{dE_M} = \left(\frac{d\Gamma}{dE_M}\right)_{\mathrm{Eq. (13)}} + \left(\frac{d\Gamma}{dE_M}\right)_g + \left(\frac{d\Gamma}{dE_M}\right)_{gg}, \tag{48}$$

with the first term interpreted according to the replacement rules given explicitly in Eqs. (27)–(31), while the last two terms are given at leading order in $\alpha_s(\sqrt{\Lambda m_b})$ in Eqs. (44) and (47) and to all orders in Appendix B.

V. PHENOMENOLOGY

We are now ready to use the expressions for CP averaged branching ratios and direct CP asymmetries derived in the previous two sections for quantitative analysis. We split the discussion into two parts, first focusing on the decays to nonisosinglet pseudoscalar and to vector final states and then moving to the predictions for the $B \to \eta X$, $\eta'X$ decays.

While the first measurements of $B \to MX$ decays have become available, one still lacks enough experimental information to determine nonperturbative charming penguin parameters from data (or to show decisively that they are small and compatible with zero). Therefore we collect in Tables III and IV only purely perturbative predictions for $B \to XM$ decay rates and direct CP asymmetries using Eqs. (15) and (16), setting the nonperturbative charming penguins parameters p_{cc}^M and $\mathcal{P}_{cc}^M$ to zero. Comparison with data then gives an insight about the importance of non-

TABLE III. Predictions for decay rates and direct CP asymmetries for charged $B^- \to MX$ $\Delta S = 1$ semi-inclusive hadronic decays, which are the same as for corresponding $\bar{B}^0 \to MX$, $\bar{B}_s^0 \to MX$ given in Table I. The first errors are an estimate of the $1/m_b$ corrections, while the second errors are due to errors on the Gegenbauer coefficients in the expansion of the LCDA.

MX	$\mathrm{Br}(B^- \to MX)/\mathrm{Br}(B \to X_s\gamma)$	A_{CP}
$K^- X_{u\bar{u}}^0$	$0.17 \pm 0.09 \pm 0.06$	$0.30 \pm 0.16 \pm 0.01$
$\bar{K}^0 X_{d\bar{u}}^-$	$0.20 \pm 0.11 \pm 0.06$	$(9.7 \pm 4.8 \pm 0.6) \times 10^{-3}$
$\pi^0 X_{s\bar{u}}^-$	$(1.0 \pm 0.6 \pm 0.2) \times 10^{-2}$	—
$K^{*-} X_{u\bar{u}}^0$	$0.28 \pm 0.16 \pm 0.06$	$0.32 \pm 0.16 \pm 0.02$
$\bar{K}^{0*} X_{d\bar{u}}^-$	$0.34 \pm 0.19 \pm 0.07$	$(8.4 \pm 4.6 \pm 1.9) \times 10^{-3}$
$\phi X_{s\bar{u}}^-$	$0.22 \pm 0.13 \pm 0.03$	$(8.9 \pm 5.0 \pm 1.6) \times 10^{-3}$
$\omega X_{s\bar{u}}^-$	$(2.8 \pm 3.3 \pm 0.7) \times 10^{-3}$	$0.49 \pm 0.24 \pm 0.33$
$\rho^0 X_{s\bar{u}}^-$	$(2.4 \pm 1.4 \pm 0.5) \times 10^{-2}$	—

TABLE IV. Predictions for decay rates and direct CP asymmetries for charged $B^- \to MX$ $\Delta S = 0$ semi-inclusive hadronic decays, which are the same as for corresponding $\bar{B}^0 \to MX$, $\bar{B}_s^0 \to MX$ given in Table II. The first errors are an estimate of the $1/m_b$ corrections, while the second errors are due to errors on the Gegenbauer coefficients in the expansion of the LCDA.

MX	$\mathrm{Br}(B^- \to MX)/\mathrm{Br}(B \to X_s\gamma)$	A_{CP}
$\pi^- X_{u\bar{u}}^0$	$0.67 \pm 0.37 \pm 0.14$	$-0.04 \pm 0.02 \pm 0.01$
$\pi^0 X_{d\bar{u}}^-$	$(4.1 \pm 2.1 \pm 2.6) \times 10^{-3}$	$0.64 \pm 0.10 \pm 0.10$
$K^0 X_{s\bar{u}}^-$	$(1.0 \pm 0.5 \pm 0.3) \times 10^{-2}$	$-0.15 \pm 0.11 \pm 0.01$
$\rho^- X_{u\bar{u}}^0$	$1.76 \pm 0.97 \pm 0.38$	$-0.04 \pm 0.02 \pm 0.01$
$\rho^0 X_{d\bar{u}}^-$	$(1.3 \pm 0.6 \pm 0.7) \times 10^{-2}$	$0.63 \pm 0.10 \pm 0.10$
$K^{*0} X_{s\bar{u}}^-$	$(1.4 \pm 0.8 \pm 0.5) \times 10^{-2}$	$-0.17 \pm 0.11 \pm 0.03$
$\phi X_{d\bar{u}}^-$	$(2.0 \pm 1.1 \pm 0.1) \times 10^{-4}$	—
$\omega X_{d\bar{u}}^-$	$(3.8 \pm 1.8 \pm 1.1) \times 10^{-3}$	$-0.72 \pm 0.13 \pm 0.20$

perturbative charming penguin contributions and/or on the size of subleading terms as detailed below Eqs. (50) and (51). To reduce the hadronic uncertainties, the predictions for $B \to XM$ branching ratios are normalized to $d\Gamma(B \to X\gamma)/dE_\gamma$. The predicted ratio of partial decay widths, Eq. (15), depends on the light meson energy E_M. In the endpoint region, however, the dependence on $x_M = 2E_M/m_B = 1 + (m_M^2 - p_X^2)/m_B^2$ is a subleading effect.[2] We neglect this dependence and set $x_M = 1$ in Tables III and IV.

For the coefficients in the Gegenbauer polynomial expansion of the LCDAs

$$\phi_M(u, \mu) = 6u\bar{u}\left[1 + \sum_{n=1}^{\infty} a_n^M(\mu) C_n^{3/2}(2u - 1)\right], \quad (49)$$

---

[2]For instance, the same p_X^2 cut corresponds to higher E_M cut for heavier mesons. For $p_X^2 < (2 \text{ GeV})^2$ one has $E_\pi > 2.26$ GeV for $B \to \pi X$, while $E_\phi > 2.36$ GeV for $B \to \phi X$ (to be compared with $m_{B^0}/2 = 2.64$ GeV). Thus $m_B/2 - E_M \sim \Lambda$ with $1 - x_M \sim O(\Lambda/m_B)$.

we take the same values as Ref. [5], except for the first coefficient in the Gegenbauer expansion of $\phi_K(x)$ for which we use the recent lattice QCD determination $a_1^K(\mu = 2.0 \text{ GeV}) = 0.055 \pm 0.005$ [34]. Explicitly, the remaining coefficients are (at $\mu = 2$ GeV): $a_2^K = 0.23 \pm 0.23$ [35], $a_1^{K^*} = 0.08 \pm 0.13$, [36], $a_2^\pi = 0.09 \pm 0.15$ [37], $a_2^{K^*} = 0.07 \pm 0.08$, $a_2^\rho = 0.14 \pm 0.15$, $a_2^\phi = 0. \pm 0.15$ [36], and for lack of better information $a_2^{\eta_q} = a_2^{\eta_s} = a_2^\pi$ and $a_2^\omega = 0. \pm 0.2$, with the higher coefficients in the expansion set to zero.

Direct CP asymmetries, Eq. (16), are nonzero only in the presence of nonzero strong phases. These can be generated nonperturbatively or by integrating out on-shell light quarks in a loop when matching full QCD to SCET_I at NLO in α_s. As in Ref. [5] we therefore use the NLO matching expressions for the Wilson coefficients $\mathcal{C}_i^p$ at $\mu = m_b$, to have the leading contribution to the CP asymmetries, while performing the evolution to the hard-collinear scale $\mu_0 \sim \sqrt{\Lambda m_b}$ at next-to-leading logarithm (NLL). Note that this running cancels to a large extent in the ratios of the decay rates (only the running of $a_n^M(\mu)$, $n \geq 1$ remains), giving in effect the Wilson coefficients with NLO accuracy at the hard-collinear scale μ_0 [5]. We choose $\mu_0 = 2$ GeV for the perturbative predictions in Tables III and IV.

The two errors quoted in Tables III and IV are an estimate of subleading corrections and due to the errors on the Gegenbauer polynomial coefficients in the LCDA expansion (49). Since the predictions are made to NLO in $\alpha_s(m_b)$ but only to LO in $1/m_b$, the largest corrections are expected to arise from the $1/m_b$ terms. These are estimated by independently varying the magnitudes of the leading terms proportional to $\lambda_{u,c,t}^{(q)}$ by 20% $\sim O(\Lambda/m_b)$ and the strong phase by 5°. This latter variation estimates the error on the strong phase arising from the uncalculated $\alpha_s(m_b)/m_b$ or $\alpha_s^2(m_b)$ terms. A 100% error is assigned to predictions for branching ratios in color-suppressed tree and QCD penguin-dominated $\Delta S = 0$ decays where the $1/m_b$ corrections are sizable compared to the leading results due to the hierarchy of Wilson coefficients. No prediction on CP asymmetries is given for these modes or for the QCD penguin-dominated $\Delta S = 1$ decays.

Next we confront the perturbative predictions with experimental data. Normalizing the *BABAR* results on semi-inclusive $B \to KX$ branching ratios, Eq. (1), to $\mathrm{Br}(B \to X_s\gamma) = (172 \pm 21) \times 10^{-6}$ with the same photon energy cut $E_\gamma > 2.34$ GeV that was used for the kaon momentum [38], one has

$$\frac{\Gamma(B^-/\bar{B}^0 \to K^- X)}{\Gamma(B \to X_s\gamma)} = 1.13 \pm 0.30, \quad (50)$$

$$\frac{\Gamma(B^-/\bar{B}^0 \to \bar{K}^0 X)}{\Gamma(B \to X_s\gamma)} = 0.89 \pm 0.42. \quad (51)$$

The central values of the measurements are substantially higher than the perturbative predictions for $B^- \to K^- X^0_{u\bar{u}}$ and $B^- \to \bar{K}^0 X^-_{d\bar{u}}$ modes,[3] given in Table III. They are still consistent within errors, with the discrepancies, respectively, at 3σ and 1.6σ levels for K^+X and K^0X modes, but do indicate that there might be substantial nonperturbative charming penguin contributions (or very large $1/m_b$ corrections). Using isospin symmetry the charming penguin parameters, p^K_{cc} and $\mathcal{P}^K_{cc}$, in the two modes are the same. The three real parameters, $|p^K_{cc}|$, $\arg(p^K_{cc})$, and $\mathcal{P}^K_{cc}$, can then be determined from the four observables: the two branching ratios (50) and (51) and the corresponding CP asymmetries once these are measured. This would also leave one observable as a consistency check.

Since the CP asymmetries are not measured yet, this procedure is not possible at present without further approximations. Quite generally one expects that roughly $|p^K_{cc}|^2 \sim \mathcal{P}^K_{cc}$. As a starting point we thus take this relation to be exact and then extract $|p^K_{cc}|$ as a function of $\arg(p^K_{cc})$ from the K^+X (K^0X) decay width. This gives for the nonperturbative charming penguin to be about a factor 4 ± 3 (4.5 ± 2) larger then the perturbative prediction, i.e. the part of C^c_4 containing the C_1 Wilson coefficient.

Here the error is a sum of the experimental error and the error due to the variation of $\arg(p^K_{cc}) \in [0, 2\pi)$. Another way of presenting this result is through the ratio of nonperturbative and perturbative contributions to the decay width

$$\left| \frac{\lambda^{(s)}_c p^K_{cc}}{h^{(s)}_K} \right| = \begin{cases} 2.2 \pm 1.1: K^+X \\ 2.0 \pm 1.5: K^0X, \end{cases} \qquad (52)$$

that should be zero if the charming penguins are purely perturbative. The error on the ratios mostly reflects the variation due to a scan over the phase of p^K_{cc}. These values are very sensitive on the assumed relation between $|p^K_{cc}|^2$ and $\mathcal{P}^K_{cc}$ and should be taken as a rough guide only. Nevertheless, they show that there is experimentally a possible indication for sizable nonperturbative charming penguin. Two ingredients would help to clarify the situation significantly. First, the inclusion of chirally enhanced $1/m_b$ terms would show whether part of the discrepancy can be attributed to those terms [22,23]. Second, the cut on $p^*(K)$ should be lowered experimentally below the rather high value of 2.34 GeV used at present [1], so that one would be sure that the measurement is in the endpoint region, where our calculations are applicable, and away from the resonance region.

Further tests are possible once more modes are measured. For instance, by using SU(3) flavor symmetry the charming penguin parameters for different modes can be related to only three real parameters, $|p_{cc}|$, $\arg(p_{cc})$, and $\mathcal{P}_{cc}$, making the framework even more predictive (at the expense of some accuracy due to SU(3) breaking). Note that in order to realize experimentally whether there are nonperturbative charming penguins and/or large $1/m_b$ corrections one does not need any symmetry arguments, just a comparison between our perturbative predictions and the experiment. To distinguish between the two sources of corrections, however, the flavor symmetries would most likely be needed.

An interesting set of modes that could be used to settle the question concerning large $1/m_b$ corrections versus nonperturbative charming penguin are the decays where no charming penguins are present. These are the $\Delta S = 0$ decay $B \to \phi X$ and the color-suppressed $\Delta S = 1$ decays $B \to \omega X$, $\pi^0 X$. They are experimentally more challenging since one would also need to measure the strangeness content of the inclusive jet. Namely, the related decays, the $\Delta S = 1$ decay $B \to \phi X$ and the $\Delta S = 0$ decays $B \to \omega X$, $\pi^0 X$, do contain charming penguins and should thus be distinguished experimentally from the first set of modes that does not contain charming penguins. Furthermore, the decays that do not receive charming penguin contributions might have substantial $1/m_b$ corrections [5], so one may need to go one higher order in the $1/m_b$ expansion to have a definite understanding of experimental results.

We next move to the decays involving η and η' mesons. The expressions for the decay widths in the endpoint region have been derived in Sec. IV with the final result given in Eq. (48). At LO in $1/m_b$, two new shape functions appear that are specific to $B \to \eta^{(\prime)} X$ decays. At lowest order in α_s, $\mathcal{S}_g(E_M, \mu_0)$ and $\mathcal{S}_{gg}(E_M, \mu_0)$ defined in Eqs. (43) and (46) (or $\mathcal{F}^M_g$ and $\mathcal{F}^M_{gg}$ in Eqs. (B17) and (B20) to all orders in α_s) describe gluonic contributions coming from one and two $\mathcal{O}_{1g}$ operator insertions, respectively, cf. Fig. 5. Little is known about these new nonperturbative functions, because of the lack of experimental data. At present only the $B \to \eta' X$ partial decay width with $E_{\eta'} > 2.218$ GeV cut has been measured [2–4]. Normalizing to the $B \to X\gamma$ decay width with the same E_γ cut gives[4]

$$\frac{\Gamma(B \to \eta' X)}{\Gamma(B \to X_s \gamma)} = 1.76 \pm 0.40. \qquad (53)$$

In $B \to \eta^{(\prime)} X$ decays there are 8 observables that are independent at LO in $1/m_b$: the $\Delta S = 1$ and $\Delta S = 0$ $B \to \eta' X$, ηX decay widths and direct CP asymmetries. Working at LO in $\alpha_s(\sqrt{\Lambda m_b})$ and neglecting the E_M de-

---

[3]The measurements are an average over charge and neutral B decays to $K^- X$ (or $\bar{K}^0 X$) final state, but these are the same to the order we are working, see Table I. Decays to $\bar{K}^0 X$ final state include also an incoherent sum with $\Delta S = 0$ decays into $K^0 X_{s\bar{u}}$, which are, however, CKM suppressed and thus small, see Table IV.

[4]If instead the same $p_{\eta'}$ and p_γ cuts are used the decay widths ratio is 1.34 ± 0.30. The difference compared to Eq. (53) reflects the effect of the large $m_{\eta'}$ mass.

TABLE V. Predictions for decay rates and direct *CP* asymmetries for charged $B^- \to \eta X^-$, $\eta' X^-$ decays $\Delta S = 1(0)$ semi-inclusive hadronic decays given in the first (last) two rows. The predictions equal also the corresponding $\bar{B}^0 \to \eta X$, $\eta' X$, $\bar{B}^0_s \to \eta X$, $\eta' X$ decay as given in Table II. The first errors are an estimate of the $1/m_b$ corrections, while the second errors are due to errors on the Gegenbauer coefficients in the expansion of the LCDA.

MX	$\mathrm{Br}(B^- \to MX)/\mathrm{Br}(B \to X_s \gamma)$	A_{CP}
$\eta X^-_{s\bar{u}}$	$(5.6 \pm 2.9 \pm 0.6) \times 10^{-2}$	$(-7.1 \pm 1.8 \pm 2.8) \times 10^{-2}$
$\eta' X^-_{s\bar{u}}$	$(1.0 \pm 2.0 \pm 0.3) \times 10^{-2}$	$0.19 \pm 0.19 \pm 0.08$
$\eta X^-_{d\bar{u}}$	$(6.2 \pm 3.2 \pm 1.3) \times 10^{-2}$	$-0.38 \pm 0.10 \pm 0.10$
$\eta' X^-_{d\bar{u}}$	$(2.4 \pm 1.2 \pm 0.7) \times 10^{-2}$	$-0.46 \pm 0.12 \pm 0.10$

pendence of shape functions, one introduces only two new nonperturbative parameters specific to these decays, $\mathcal{S}_g$ and $\mathcal{S}_{gg}$. With more data they could in principle be determined from experiment in the future. Note, in particular, that the charming penguin parameters entering the predictions can be fixed using SU(3) flavor symmetry from semi-inclusive decays into nonisosinglets.

To have some future guidance on the size of the missing components, we list in Table V the purely perturbative predictions where we set both the charming penguin as well as the new gluonic shape function contributions to zero and neglect NLO corrections from $\mathcal{O}_{2g}$ insertions. One striking aspect of that calculation is that the prediction for $\Delta S = 1$ $B \to \eta' X_s$ decay falls remarkably short of the large measured value. Furthermore in this incomplete perturbative prediction the hierarchy between ηX_s and $\eta' X_s$ decays is exactly opposite to the one found in two-body $B \to \eta' K$, ηK decays. While $\mathrm{Br}(B \to \eta' K) \gg \mathrm{Br}(B \to \eta K)$, the hierarchy in the incomplete prediction for the semi-inclusive decays is inverted. In the two-body decays the hierarchy is well explained through the constructive and destructive interference of $B \to \eta_q K$ and $B \to \eta_s K$ contributions in $B \to \eta' K$ and $B \to \eta K$ amplitudes, respectively, due to $\eta - \eta'$ mixing, if $A(B \to \eta_q K) \simeq A(B \to \eta_s K)$. This is exactly what is found in the limit of charming penguin dominance [21,39]. In the semi-inclusive decay on the other hand there are no charming penguin contributions to $B \to \eta_q X_s$ at LO in $1/m_b$, cf. Eq. (30), so that with large charming penguins there is no large hierarchy between $B \to \eta' X_s$ and $B \to \eta X_s$ decays.

To be more quantitative, it is instructive to take three formal limits: (i) dominating charming penguins, (ii) dominating $\mathcal{O}_{2g}$ contributions, and (iii) the incomplete perturbative prediction with $\mathcal{C}_{2g} \to 0$. If the amplitudes are dominated by charming penguins then (in the SU(3) symmetric limit)

$$\frac{\mathrm{Br}(B^- \to \eta X^-_{s\bar{u}})}{\mathrm{Br}(B^- \to \eta' X^-_{s\bar{u}})} = \tan^2 \phi = 0.67. \quad (54)$$

Thus, as already argued above, in this limit there is no hierarchy between the two decays since Lipkin's argument of destructive and constructive interferences does not work for semi-inclusive decays. On the other hand, if $\mathcal{O}_{2g}$ contributions dominate then working at LO in $\alpha_s(\sqrt{\Lambda m_b})$ we have

$$\frac{\mathrm{Br}(B^- \to \eta X^-_{s\bar{u}})}{\mathrm{Br}(B^- \to \eta' X^-_{s\bar{u}})}$$
$$= \frac{|(\cos\phi f_{\eta_q} \phi_{\eta_q} - \sin\phi f_{\eta_s} \phi_{\eta_s}) \otimes (\frac{1}{u} + \frac{1}{\bar{u}})|^2}{|(\cos\phi f_{\eta_q} \phi_{\eta_q} + \sin\phi f_{\eta_s} \phi_{\eta_s}) \otimes (\frac{1}{u} + \frac{1}{\bar{u}})|^2}. \quad (55)$$

Numerically this gives 1.2×10^{-4} if asymptotic LCDA are used, and 1.52×10^{-2} if SU(3) breaking is estimated by setting $a_2^{\eta_s} = a_2^K$ instead. In the limit of dominant $\mathcal{O}_{2g}$ contributions we thus have a similar large hierarchy between ηX_s and $\eta' X_s$ decays as in the two-body decays due to the destructive interference as is apparent from Eq. (55). Finally, if the incomplete perturbative calculation were a valid approximation, then we would have an inverted hierarchy between ηX_s and $\eta' X_s$ decays. This is due to a cancellation that is found between different terms in the $B \to \eta' X_s$ perturbative prediction. Because of small $B \to \eta' X_s$ decay width, however, this limit is phenomenologically excluded.

In order to understand the relative size of charming penguin and the $\mathcal{O}_{2g}$ contributions it is important to have a measurement of $B \to \eta X_s$ decays. The relative size compared to the $B \to \eta' X_s$ decay width is clearly different in the two extreme cases when only one of the two contributions is important. Comparing further with the other decays one should be able to determine all the nonperturbative parameters. As an exercise we set $\mathcal{P}^{\eta_s} = |p^{\eta_s}_{cc}|^2$ and take $p^{\eta_s}_{cc}$ to be equal to p^K_{cc} obtained from $B \to K^- X$, leading to a prediction for the normalized decay width $\mathrm{Br}(B^- \to \eta' X^-_{s\bar{u}})/\mathrm{Br}(B \to X_s \gamma) = 0.43 \pm 0.25$ with the variation mainly due to the unknown strong phase of p^K_{cc} (while for the $\Delta S = 0$ decay we find $\mathrm{Br}(B^- \to \eta' X^-_{d\bar{u}})/\mathrm{Br}(B \to X_s \gamma) = 0.02 \pm 0.02$). This is still smaller then the measured value (53), not surprising given the approximations made to arrive at it. Whether the difference is partially explained also by $\mathcal{O}_{2g}$ contributions should be clarified once more data are available.

VI. CONCLUSIONS

In the framework of SCET we considered semi-inclusive, hadronic decays $B \to XM$ in the endpoint region, where the light meson M and the inclusive jet X with $p_X^2 \sim \Lambda m_b$ are emitted back to back. This is an extension of the analysis done in Ref. [5] where we limited consideration to decays in which the spectator quark does not enter into the meson M. The contributions in which the spectator quark enters the meson M are power suppressed by $1/m_b^2$ in SCET. In this work we thus extend the SCET

predictions at LO in $1/m_b$ to all decays where the spectator can enter either the jet X or the meson M. In SCET the four-quark operators factorize, which allows for a systematic theoretical treatment. After matching the full QCD effective weak Hamiltonian onto SCET$_I$, the weak interaction four-quark operators factor into the heavy-to-light current and the $\bar{n}$-collinear current. The forward scattering amplitude of the heavy-to-light currents leads to a convolution $\mathcal{S}$ of the jet function with the B-meson shape function, while the matrix element of $\bar{n}$-collinear currents gives the LCDA for the meson M. The product of the two then gives the factorized form for the decay rates. The two nonperturbative functions, the convolution $\mathcal{S}$ and the LCDA, are the only nonperturbative inputs in the predictions for $B \to XM$ decay rates at leading order in $1/m_b$. Furthermore, the same convolution $\mathcal{S}$ appears in $B \to X_s \gamma$ decay and drops out in the ratio of $B \to XM$ to the $B \to X_s \gamma$ rate and in the predictions for direct CP asymmetries. Further work on higher-order corrections would be useful in reducing the theoretical uncertainty.

Nonperturbative charming penguin contributions can be included by the addition of one real and one complex parameter in the SU(3) symmetry limit. These parameters, which are zero if the charming penguins are purely perturbative, can in principle be extracted from data. Thus by investigating decays without charming penguins, we can test whether the formalism is working. Then by looking at modes where the charming penguin can contribute, we can potentially see whether or not the charming penguin gives a large contribution to the decays.

Decays where the light meson is an isosinglet η or η' are special in that they receive additional contributions from gluonic operators. We consider these decays in detail, and show that the decay rate still factorizes, but there are two new shape functions which enter into the predicted rate.

Using the available data, we performed an analysis of the semi-inclusive hadronic decays. While to date the data is limited, our preliminary analysis seems to indicate either large higher-order corrections or a large contribution from nonperturbative charming penguins. With more data, it may be possible to distinguish the two possibilities as well as to extract the size of the nonperturbative charming penguin contributions.

ACKNOWLEDGMENTS

APPENDIX A: TREE-LEVEL MATCHING

The matching of the effective weak Hamiltonian in full QCD

$$H_W = \frac{G_F}{\sqrt{2}} \Bigg[\sum_{p=u,c} \lambda_p^{(q)} (C_1 O_1^p + C_2 O_2^p)$$
$$- \lambda_t^{(q)} \Bigg(\sum_{i=3}^{10} C_i O_i + C_g O_g + C_\gamma O_\gamma \Bigg) \Bigg], \quad \text{(A1)}$$

onto an SCET$_I$ one was calculated at NLO in $\alpha_s(m_b)$ first in Refs. [23], and then in Ref. [19], giving the SCET$_I$ effective weak Hamiltonian in Eq. (7). Here we list for reader's convenience the tree-level result of the matching

$$\mathcal{C}_{1,2}^p(v) = \delta_{up} \Bigg[C_{1,2} + \frac{C_{2,1}}{N} \Bigg] + \frac{3}{2} \Bigg[C_{10,9} + \frac{C_{9,10}}{N} \Bigg],$$
$$\mathcal{C}_3^p(v) = \frac{3}{2} \Bigg[C_7 + \frac{C_8}{N} \Bigg],$$
$$\mathcal{C}_{4,5}^p(v) = C_{4,3} + \frac{C_{3,4}}{N} - \frac{1}{2} \Bigg[C_{10,9} + \frac{C_{9,10}}{N} \Bigg], \quad \text{(A2)}$$
$$\mathcal{C}_6^p(v) = C_5 + \frac{C_6}{N} - \frac{1}{2} \Bigg[C_7 + \frac{C_8}{N} \Bigg],$$

while the NLO results in our notation can be found in Appendix A of Ref. [5].

APPENDIX B: DERIVATION OF GLUONIC CONTRIBUTIONS

In this appendix we provide details on the derivation of $\mathcal{G}(0)$ in Eq. (35) and extend the results for $(d\Gamma/dE_M)_g$ and $(d\Gamma/dE_M)_{gg}$ in Eqs. (44) and (47) to all orders in $\alpha_s(\sqrt{\Lambda m_b})$. We start with the T-products

$$\mathcal{G}_{\xi\xi(cg)} = \langle MX| i \int d^4x T\{\mathcal{O}_{1g}(0), \mathcal{L}_{\xi\xi(cg)}^{(1)}(x)\}|B\rangle, \quad \text{(B1)}$$

that were already defined in Eq. (32) and are also shown in Fig. 6. The subleading SCET Lagrangians appearing in Eq. (B1) are

$$\mathcal{L}_{\xi\xi}^{(1)} = \bar{q}_{\bar{n}}' (Y_{\bar{n}}^\dagger i \not{D}_{us}^\perp Y_{\bar{n}}) \frac{1}{n \cdot P} (W_{\bar{n}}^\dagger i \not{D}_{\bar{n}}^\perp W_{\bar{n}}) \frac{\not{n}}{2} q_{\bar{n}}'$$
$$+ \bar{q}_{\bar{n}}' (W_{\bar{n}}^\dagger i \not{D}_{\bar{n}}^\perp W_{\bar{n}})(Y_{\bar{n}}^\dagger i \not{D}_{us}^\perp Y_{\bar{n}}) \frac{1}{n \cdot P} \frac{\not{n}}{2} q_{\bar{n}}', \quad \text{(B2)}$$

where the sum over light quark flavors q' is understood, and [40]

$$\mathcal{L}_{cg}^{(1)} = \frac{2}{g^2} \text{Tr}\{[iD_0^\mu, iD_c^{\perp\nu}][iD_{0\mu}, W_{\bar{n}} iD_{us\nu}^\perp W_{\bar{n}}^\dagger]\}, \quad \text{(B3)}$$

with $iD_0^\mu = i\mathcal{D}^\mu + gA_{\bar{n}}^\mu$ and $i\mathcal{D}^\mu = \frac{\bar{n}^\mu}{2}P + P_\perp^\mu + \frac{n^\mu}{2}i\bar{n}\cdot D_{\text{us}}$.

For the calculation of $\mathcal{G}_{\xi\xi}$ it is useful to rewrite

$$
\begin{aligned}
\mathcal{L}_{\xi\xi}^{(1)} &= \mathcal{L}_{\xi\xi,a}^{(1)} + \mathcal{L}_{\xi\xi,b}^{(1)} \\
&= \bar{q}_{\bar{n}}' g\,\mathcal{A}_{\text{us}}^\perp \frac{1}{n\cdot P}\,ig\mathcal{B}_{\bar{n}}^\perp \frac{\slashed{n}}{2} q_{\bar{n}}' + \bar{q}_{\bar{n}}'\,ig\mathcal{B}_{\bar{n}}^\perp g\,\mathcal{A}_{\text{us}}^\perp \frac{1}{n\cdot P} \\
&\quad \times \frac{\slashed{n}}{2} q_{\bar{n}}' + \ldots,
\end{aligned} \tag{B4}
$$

with $\mathcal{A}_{\text{us}}^{\perp\mu}$ defined in Eq. (34), while the ellipses denote additional terms containing $P_\perp$ that do not contribute in our case. $\mathcal{G}_{\xi\xi}$ is then also split accordingly into

$$
\mathcal{G}_{\xi\xi,a(b)} = \langle MX|i\int d^4x\,T\{\mathcal{O}_{1g}(0), \mathcal{L}_{\xi\xi,a(b)}^{(1)}(x)\}|B\rangle. \tag{B5}
$$

In the SCET$_\text{I}$ to SCET$_\text{II}$ matching (where $p^2 \sim \Lambda m_b$ intermediate degrees of freedom are integrated out) we focus on the $\bar{n}$ fields in $\mathcal{G}_{\xi\xi,a}$. The matching leads to two jet functions once hard-collinear modes are integrated out, and we obtain

$$
\begin{aligned}
&T\{[\mathcal{B}_{\bar{n}}^{\perp\mu}]^{cd}(0), [(\bar{q}_{\bar{n}})^a(\gamma_\perp^\alpha \mathcal{B}_{\bar{n}}^\perp \slashed{n} q_{\bar{n}})^b]_u(x)\} \\
&= i\delta(x_-)\delta^2(x_\perp)\frac{1}{m_b}\int \frac{dk_-}{2\pi} e^{-ik_- x_+/2}[(T^A)^{ba} \\
&\quad \times (T^A)^{cd}J_1(u, k_-) + \delta^{ab}\delta^{cd}J_1'(u, k_-)] \\
&\quad \times [\bar{q}_{\bar{n}}\gamma_\perp^\alpha \gamma_\perp^\mu \slashed{n} q_{\bar{n}}]_u + \cdots,
\end{aligned} \tag{B6}
$$

with $k_- = \bar{n}\cdot k$, $x_+ = n\cdot x$. The ellipses are terms which do not contribute to $\eta^{(\prime)}$ states. Tree-level matching gives for the jet functions $J_1(u, k_-) = 1/(Nk_-)$ and $J_1'(u, k_-) = 0$. The J_1' term does not contribute to $\mathcal{G}_{\xi\xi,a}$ since it leads to $\text{Tr}(g\mathcal{A}_{\text{us}}^{\perp\mu}) = 0$. The remaining piece can be rearranged using color identities into

$$
\begin{aligned}
\mathcal{G}_{\xi\xi,a} &= \frac{\alpha_s}{4\pi}\int \frac{dk_-dx_+}{4\pi}e^{-ik_- x_+/2}\int du\frac{J_1(u, k_-)}{u} \\
&\quad \times \langle MX|[\bar{q}_n\slashed{n}\gamma_\mu^\perp P_R Y_n^\dagger Y_{\bar{n}} g\,\mathcal{A}_{\text{us}\alpha}^\perp(x)Y_{\bar{n}}^\dagger b_v] \\
&\quad \times [\bar{q}_{\bar{n}}\gamma_\perp^\alpha \gamma_\perp^\mu \slashed{n} q_{\bar{n}}]_u|B\rangle.
\end{aligned} \tag{B7}
$$

The two terms in the square brackets are factorized in the sense that there are no soft gluon exchanges between the two terms—all the soft fields are in the first bracket. The communication between the two is only through the k_- and u convolutions with the jet function $J_1(u, k_-)$.

Using the definition of the LCDA

$$
\langle M|(q_{\bar{n}})_i^a[(\bar{q}_{\bar{n}})_j^b]_u|0\rangle = -\frac{i}{2}E_M f_M\phi_M(u)\frac{\delta^{ab}}{N}\left(\frac{\slashed{n}}{2}\gamma_5\right)_{ij}, \tag{B8}
$$

to evaluate the matrix element from the second square bracket in (B7) we then have

$$
\begin{aligned}
\mathcal{G}_{\xi\xi,a} &= -\frac{i\alpha_s m_b}{4\pi}\int du f_M\phi_M(u) \\
&\quad \times \int \frac{dk_-dx_+}{4\pi}e^{-ik_- x_+/2}\frac{1}{u}J_1(u, k_-) \\
&\quad \times \langle X|\bar{q}_n Y_n^\dagger Y_{\bar{n}}(0)\slashed{n}g\,\mathcal{A}_{\text{us}}^\perp(x_+)P_R Y_{\bar{n}}^\dagger b_v(0)|B\rangle.
\end{aligned} \tag{B9}
$$

In simplifying the Dirac structure the identity

$$
\epsilon_\perp^{\alpha\mu}[\slashed{n}, \slashed{\bar{n}}]\gamma_{\perp\mu}P_R = 4i\gamma_\perp^\alpha P_R \tag{B10}
$$

was used, $\epsilon^{0123} = +1$, and $\epsilon_\perp^{\alpha\mu} = \epsilon^{\alpha\mu\lambda\sigma}\bar{n}_\lambda n_\sigma/2$. For the derivation of $\mathcal{G}_{\xi\xi,b}$ we notice that $\mathcal{L}_{\xi\xi,b}^{(1)}$ is a Hermitian conjugate of $\mathcal{L}_{\xi\xi,a}^{(1)}$. Using the Hermitian conjugate of (B6) we finally have

$$
\begin{aligned}
\mathcal{G}_{\xi\xi} &= -\frac{i\alpha_s m_b}{4\pi}\int du f_M\phi_M(u)\int \frac{dk_-dx_+}{4\pi}e^{-ik_- x_+/2} \\
&\quad \times \left(\frac{1}{u}J_1(u, k_-) - \frac{1}{\bar{u}}J_1(\bar{u}, -k_-)^*\right) \\
&\quad \times \langle X|\bar{q}_n Y_n^\dagger Y_{\bar{n}}(0)\slashed{n}g\,\mathcal{A}_{\text{us}}^\perp(x_+)P_R Y_{\bar{n}}^\dagger b_v(0)|B\rangle.
\end{aligned} \tag{B11}
$$

Moving now to the calculation of $\mathcal{G}_{cg}$, we first rewrite $\mathcal{L}_{cg}^{(1)}$ in a more useful form

$$
\mathcal{L}_{cg}^{(1)} = \frac{2}{g^2}\text{Tr}\{[ig\mathcal{B}_{\bar{n}\perp}^\mu, ig\mathcal{B}_{\bar{n}\perp}^\nu][ig\mathcal{B}_{\bar{n}\mu}^\perp, g\,\mathcal{A}_{\text{us}\nu}^\perp]\} + \cdots, \tag{B12}
$$

where the ellipses denote terms that do not contribute to $\mathcal{G}_{cg}$. The matching from SCET$_\text{I}$ to SCET$_\text{II}$ gives

$$
\begin{aligned}
&T\{ig(\mathcal{B}_{\bar{n}\perp}^\mu)^{cd}(0), \mathcal{L}_{cg}^{(1)}(x)\} \\
&= i\epsilon_\perp^{\mu\nu}g(\mathcal{A}_{\text{us}\nu}^\perp)^{cd}(x)\delta(x_-)\delta^2(x_\perp)\int \frac{dk_-}{2\pi}e^{-ik_- x_+/2}\frac{1}{m_b} \\
&\quad \times \int du J_g(u, k_-)\epsilon_\perp^{\mu'\nu'}\text{Tr}[ig\mathcal{B}_{\bar{n}\mu'}^\perp ig\mathcal{B}_{\bar{n}\nu'}^\perp]_u + \cdots,
\end{aligned} \tag{B13}
$$

where again the ellipses denote terms that do not contribute for $\eta^{(\prime)}$ final states either because the collinear gluons are not in color-singlet combination or they have incorrect parity. Using the definition of gluonic LCDA Eq. (21) and the identity (B10), we then have

$$
\begin{aligned}
\mathcal{G}_{cg} &= -i\sqrt{C_F}\frac{\alpha_s m_b}{4\pi}\int du f_P^1\bar{\Phi}_P^g(u) \\
&\quad \times \int \frac{dk_-dx_+}{4\pi}e^{-ik_- x_+/2}J_g(u, k_-) \\
&\quad \times \langle X|\bar{q}_n Y_n^\dagger Y_{\bar{n}}(0)\slashed{n}g\,\mathcal{A}_{\text{us}}^\perp(x_+)P_R Y_{\bar{n}}^\dagger b_v(0)|B\rangle.
\end{aligned} \tag{B14}
$$

At tree level we have $J_g(u, k_-) = J_g(k_-)$, independent of u. Since $\bar{\Phi}_P^g(u)$ is antisymmetric, $\bar{\Phi}_P^g(u) = -\bar{\Phi}_P^g(\bar{u})$, the matrix element $\mathcal{G}_{cg}$ vanishes at this order. The sum of the

two contributions, $\mathcal{G}_{\xi\xi}$ in Eq. (B11) and $\mathcal{G}_{cg}$ in Eq. (B14), then gives the result for $\mathcal{G}(0)$ quoted in Eq. (35).

We next extend the results for $(d\Gamma/dE_M)_g$ and $(d\Gamma/dE_M)_{gg}$ in Eqs. (44) and (47) to all orders in $\alpha_s(\sqrt{\Lambda m_b})$. To do so, we redefine the heavy-to-light current $\tilde{\mathcal{J}}$ in Eq. (38) to contain also the integration over hard momenta fractions u [since in general one may not be able to factor this dependence from the dependence on soft k_- momenta in the jet functions $J_{1,g}(u, k_-)$],

$$\mathcal{J}^M(0) = \int du \int \frac{dk_- dx_+}{4\pi} e^{-ik_- x_+/2} F^M(k_-, u)\tilde{J}_H(0, x_+).$$
(B15)

The heavy current $\tilde{J}_H$ is given in Eq. (33), while the hard-collinear kernel multiplied by LCDA, $F^M(k_-, u)$, is given in Eq. (36). Unlike the current $\tilde{\mathcal{J}}$ in Eq. (38), the current $\mathcal{J}^M$ in (B15) depends on the final state meson M through LCDA that are part of the $F^M(k_-, u)$ function.

The derivation of the $B \to XM$ decay width is now very similar to the one given in Sec. IV. Starting from the T product of heavy currents corresponding to one $\mathcal{O}_{1g}$ insertion,

$$T_g^M(E_M) = \frac{i}{m_b} \int d^4z \langle \bar{B}|TJ_H^\dagger(z)\mathcal{J}^M(0)|\bar{B}\rangle,$$
(B16)

with $J_H(z) = e^{i(\tilde{p}-m_b v)\cdot z}(\bar{q}_n \slashed{n} P_L Y_n^\dagger b_v)(z)$ and $\mathcal{J}^M(0)$ given in (B15), we use the factorization of n collinear quark fields from the rest at LO in $1/m_b$ to write

$$\text{Disc.}T_g^M(E_M) = 2 \int dl_+ dr_- \int du$$
$$\times \text{Im}\left[\frac{-1}{\pi} J_P(l_+ + m_b - 2E_M + i\epsilon)\right]$$
$$\times f_g(l_+, r_-) F^M(r_-, u)$$
$$\equiv 2\mathcal{F}_g^M(E_M, \mu_0),$$
(B17)

where the n-collinear jet function $J_P(\kappa_+ + i\epsilon)$ was defined

in Eq. (41), while the shape function $f_g(l_+, r_-)$ was defined in Eq. (42). Using the optical theorem we now have for the decay width contribution from single $\mathcal{O}_{1g}$ insertion

$$\left(\frac{d\Gamma}{dE_M}\right)_g = \frac{G_F^2}{4\pi} m_b^2 x_M^2 f_M \, 2\text{Re}[\lambda_t^{(q)} C_{1g} \mathcal{F}_g^M(E_M, \mu_0)$$
$$\times (\phi_M \otimes \lambda_p^{(q)} T_{M,p}^{(q)})^*].$$
(B18)

This extends Eq. (44) to all orders in $\alpha_s(\sqrt{\Lambda m_b})$. We reiterate that the shape function $\mathcal{F}_g^M(E_M, \mu_0)$ now contains an integral over hard momenta fractions in the LCDA so that it depends on the meson M.

Defining similarly for the double $\mathcal{O}_{1g}$ insertion

$$T_{gg}^M(E_M) = \frac{i}{m_b} \int d^4z \langle \bar{B}|T\mathcal{J}^{M\dagger}(z)\mathcal{J}^M(0)|\bar{B}\rangle,$$
(B19)

we have

$$\text{Disc.}T_{gg}^M(E_M) = 2 \int dl_+ dr_- ds_-$$
$$\times \text{Im}\left[-\frac{1}{\pi} J_P(l_+ + m_b - 2E_M + i\epsilon)\right]$$
$$\times \int du F^M(r_-, u) \int dv F^M(s_-, v)^*$$
$$\times f_{gg}(l_+, r_-, s_-)$$
$$\equiv 2m_b \mathcal{F}_{gg}^M(E_M, \mu_0),$$
(B20)

where the shape function $f_{gg}(l_+, r_-, s_-)$ that depends on three soft momenta was defined in Eq. (45). For the double $\mathcal{O}_{1g}$ insertion contribution to the decay width we then have

$$\left(\frac{d\Gamma}{dE_M}\right)_{gg} = \frac{G_F^2}{2\pi} m_b^2 x_M \mathcal{F}_{gg}^M(E_M, \mu_0)|\lambda_t^{(q)} C_{1g}|^2,$$
(B21)

which extends Eq. (47) to all orders in $\alpha_s(\sqrt{\Lambda m_b})$, with the shape function $\mathcal{F}_{gg}^M(E_M, \mu_0)$ again depending on the meson M through the LCDA.

[1] B. Aubert (*BABAR* Collaboration), arXiv:hep-ex/0607053.
[2] T. E. Browder *et al.* (CLEO Collaboration), Phys. Rev. Lett. **81**, 1786 (1998).
[3] B. Aubert *et al.* (*BABAR* Collaboration), Phys. Rev. Lett. **93**, 061801 (2004).
[4] G. Bonvicini *et al.* (CLEO Collaboration), Phys. Rev. D **68**, 011101 (2003).
[5] J. Chay, C. Kim, A. K. Leibovich, and J. Zupan, Phys. Rev. D **74**, 074022 (2006).
[6] A. Soni and J. Zupan, Phys. Rev. D **75**, 014024 (2007).
[7] C. W. Bauer, S. Fleming, and M. E. Luke, Phys. Rev. D **63**, 014006 (2000).
[8] C. W. Bauer, S. Fleming, D. Pirjol, and I. W. Stewart, Phys. Rev. D **63**, 114020 (2001).
[9] C. W. Bauer and I. W. Stewart, Phys. Lett. B **516**, 134 (2001).
[10] C. W. Bauer, D. Pirjol, and I. W. Stewart, Phys. Rev. D **65**, 054022 (2002).
[11] T. E. Browder, A. Datta, X. G. He, and S. Pakvasa, Phys. Rev. D **57**, 6829 (1998); A. Datta, X. G. He, and S. Pakvasa, Phys. Lett. B **419**, 369 (1998); X. G. He, C. P. Kao, J. P. Ma, and S. Pakvasa, Phys. Rev. D **66**, 097501 (2002).
[12] D. Atwood and A. Soni, Phys. Rev. Lett. **79**, 5206 (1997).
[13] A. L. Kagan and A. A. Petrov, arXiv:hep-ph/9707354.

[14] X. G. He and G. L. Lin, Phys. Lett. B **454**, 123 (1999); X. G. He, J. P. Ma, and C. Y. Wu, Phys. Rev. D **63**, 094004 (2001); X. G. He, C. Jin, and J. P. Ma, Phys. Rev. D **64**, 014020 (2001).

[15] X. Calmet, T. Mannel, and I. Schwarze, Phys. Rev. D **61**, 114004 (2000); **62**, 096014 (2000); X. Calmet, Phys. Rev. D **62**, 014027 (2000); **62**, 016011 (2000).

[16] H. Y. Cheng and A. Soni, Phys. Rev. D **64**, 114013 (2001).

[17] C. S. Kim, J. Lee, S. Oh, J. S. Hong, D. Y. Kim, and H. S. Kim, Eur. Phys. J. C **25**, 413 (2002).

[18] G. Eilam and Y. D. Yang, Phys. Rev. D **66**, 074010 (2002).

[19] J. Chay and C. Kim, Nucl. Phys. **B680**, 302 (2004).

[20] C. W. Bauer, D. Pirjol, I. Z. Rothstein, and I. W. Stewart, Phys. Rev. D **70**, 054015 (2004); C. W. Bauer, I. Z. Rothstein, and I. W. Stewart, Phys. Rev. D **74**, 034010 (2006).

[21] A. R. Williamson and J. Zupan, Phys. Rev. D **74**, 014003 (2006).

[22] A. Jain, I. Z. Rothstein, and I. W. Stewart, arXiv:0706.3399.

[23] M. Beneke, G. Buchalla, M. Neubert, and C. T. Sachrajda, Phys. Rev. Lett. **83**, 1914 (1999); Nucl. Phys. **B591**, 313 (2000); **B606**, 245 (2001); M. Beneke and M. Neubert, Nucl. Phys. **B675**, 333 (2003).

[24] M. Beneke and S. Jager, Nucl. Phys. **B751**, 160 (2006); **B768**, 51 (2007).

[25] M. Beneke, J. Rohrer, and D. Yang, Nucl. Phys. **B774**, 64 (2007).

[26] C. W. Bauer, D. Pirjol, and I. W. Stewart, Phys. Rev. D **66**, 054005 (2002).

[27] C. W. Bauer, D. Pirjol, and I. W. Stewart, Phys. Rev. D **67**, 071502 (2003).

[28] K. S. M. Lee and I. W. Stewart, Nucl. Phys. **B721**, 325 (2005).

[29] For a review, see e.g. G. Buchalla, A. J. Buras, and M. E. Lautenbacher, Rev. Mod. Phys. **68**, 1125 (1996).

[30] P. Kroll and K. Passek-Kumericki, Phys. Rev. D **67**, 054017 (2003).

[31] A. E. Blechman, S. Mantry, and I. W. Stewart, Phys. Lett. B **608**, 77 (2005).

[32] M. K. Chase, Nucl. Phys. **B174**, 109 (1980); S. Fleming and A. K. Leibovich, Phys. Rev. D **70**, 094016 (2004).

[33] T. Feldmann *et al.*, Phys. Rev. D **58**, 114006 (1998); Phys. Lett. B **449**, 339 (1999).

[34] P. A. Boyle *et al.* (UKQCD Collaboration), Phys. Lett. B **641**, 67 (2006); see also V. M. Braun *et al.*, Phys. Rev. D **74**, 074501 (2006).

[35] P. Ball, V. M. Braun, and A. Lenz, J. High Energy Phys. 05 (2006) 004.

[36] P. Ball and R. Zwicky, Phys. Rev. D **71**, 014029 (2005).

[37] P. Ball and R. Zwicky, Phys. Rev. D **71**, 014015 (2005).

[38] O. Buchmuller and H. Flacher, Phys. Rev. D **73**, 073008 (2006); for lower cut $E_\gamma > 2.34$ GeV the extrapolation factor is 0.485 ± 0.046, H. Flacher (private communication).

[39] H. J. Lipkin, Phys. Lett. B **254**, 247 (1991).

[40] C. W. Bauer, D. Pirjol, and I. W. Stewart, Phys. Rev. D **68**, 034021 (2003).